







## Research Article

## Design, development, and performance evaluation of a GPS and machine vision-based navigation system for an intelligent field guard robot

Jafar Massah<sup>a\*</sup> , Keyvan Asefpour Vakilian<sup>b</sup> , Soha Sami<sup>a</sup> , Iman Jazayeri<sup>a</sup> 

<sup>a</sup> Department of Agrotechnology, College of Aburaihan, University of Tehran, Tehran, I. R. Iran

<sup>b</sup> Department of Biosystems Engineering, Gorgan University of Agricultural Sciences and Natural Resources, Gorgan, I. R. Iran

## ARTICLE INFO

## Keywords:

Attacking animals  
Camera  
Control points  
GPS  
Image processing

**Received:** 21 July 2025

**Revised:** 19 November 2025

**Accepted:** 22 November 2025

**ABSTRACT-** An innovative approach to protecting farmland from wild animals is the use of an intelligent field-guard robot. In this study, a fully featured field-guard robot was designed and developed using image processing and a global positioning system (GPS). To achieve this, the robot's tracking system, which combines a machine-vision camera and a GPS receiver, was evaluated. For automatic tracking, several control points were established within an experimental field, and their latitude and longitude coordinates were provided to the robot to enable GPS-based navigation. As the robot moved through the field, it captured and processed images to detect and pursue moving objects, such as approaching or attacking animals. The performance of the tracking system, the image-processing algorithm, and the robot's ability to detect and chase animals were investigated. The results showed that the robot's tracking system performed better in sunny weather compared to cloudy and partly cloudy conditions. To evaluate the image-processing algorithm, RGB, HSV, and Lab color models were examined, and the RGB color model was found to be the most suitable. A normalized standard deviation of 10% in the image provided the best performance for detecting the attacking animals. Evaluation of the robot's performance in repelling attacking animals showed promising results, with successful repulsion of four out of five attacking animals under sunny and partly cloudy weather conditions.

## INTRODUCTION

Changing cultivation patterns in a region often leads to increased attacks by wild animals on agricultural fields. This occurs largely because agricultural land is converted into artificial forests or used for constructing temporary shelters for these animals (Vijayan & Pati, 2002). Crop damage caused by such attacks poses a significant threat to agricultural yields (Bapat et al., 2017). For example, in the Hyrcanian forests of northern Iran, rural highlands and areas located near protected zones are reported to experience more frequent wildlife incursions than other regions (Meinecke et al., 2018). Wild animal intrusions reduce both the quantity and quality of crops, and encounters between these animals and ranchers or livestock can lead to severe incidents, including human fatalities and predatory attacks. In one study conducted in Kashmir, India, from January 2005 to October 2007, a total of 203 wild animal attacks on humans were recorded, resulting in 26 deaths and 177 serious injuries. Of the victims, 145 (71.5%) were male and 58 (28.5%) were female (Nabi et al., 2009). Globally, various methods are used to deter wild animals from entering agricultural lands. A commonly

used approach to prevent injuries caused by white-tailed deer is the installation of repellent fences, although their construction and installation require relatively high costs. These fences are typically used to protect orchards, vegetable fields, and other high-value agricultural resources (Vercauteren et al., 2006). In the United States, farmers employ several strategies, including temporary electric fences, to protect their fields from deer. These electric fences come in different forms, such as peanut butter fences, polytape fences, and high-tensile electric fences, including offset, vertical, and slanted configurations (Craven & Hygnstrom, 1994). The economic benefit of using partial poly-mesh fences with 50-meter wings to prevent deer attacks is relatively low, estimated at only 205 USD per hectare per year over a 10-year period (Hildreth et al., 2012). The effectiveness of ultrasonic and other electronic deterrent devices for repelling birds has not been supported by academic studies, as birds, like humans, cannot hear frequencies above 20 kHz. Other devices, such as high-pitched sounds, explosive gas cannons, battery-operated alarms, fireworks, lights, and various triggering mechanisms, are also used to scare birds away from farmlands. Additionally, ultrasonic devices and acoustic vibration generators

\*Corresponding Author: Professor, Department of Agrotechnology, College of Aburaihan, University of Tehran, Tehran, I. R. Iran

E-mail address: [jmassah@ut.ac.ir](mailto:jmassah@ut.ac.ir)

DOI: [10.22099/iar.2026.53745.1698](https://doi.org/10.22099/iar.2026.53745.1698)



have been found ineffective for repelling kangaroo rats (Howard, 1994).

The use of robots in the modern world is increasing rapidly (Massah & Ghazavi, 2009; Hashemi et al., 2014). Advances in technology have made it possible for humans and robots to work together safely (Grahn et al., 2018). Today, robots are widely applied across various industries. For instance, wearable medical devices such as robotic exoskeletons have emerged as one of the most promising solutions for assisting individuals with movement disorders. Robot-assisted rehabilitation can reduce the workload of therapists while enabling patients to perform therapeutic exercises more effectively (Chen et al., 2020). Industrial robots are also designed to perform a wide range of operations, and their applications have recently expanded to complex tasks such as cleaning the exterior surfaces of skyscrapers (Kouzehgar et al., 2019).

Given the broad capabilities of robots in practical applications, their use represents a suitable approach for repelling attacking animals from agricultural fields. A smart field-guard robot can serve as a permanent protective system capable of operating in high-risk conditions, analyzing its environment, and responding appropriately. Such a robot can help repel wild animals and protect crops, livestock, poultry, and cattle.

Planting, fertilizing, plant protection, and harvesting are among the most important agricultural processes that can be automated (Vidović & Scitovski, 2014). In a study by Xue et al. (2012), a machine-vision technique guided by maize cultivation rows was used to track the AgBo robot, a guard robot designed for corn fields. The robot's machine-vision hardware included a camera equipped with pitch and yaw motion control. Navigation along crop rows was achieved using fuzzy-logic control. Performance evaluation of the robot's tracking system (RTK), based on global positioning system (GPS) data, demonstrated a maximum navigation error of 15.8 mm and stable navigation behavior. Vidović and Scitovski (2014) proposed an efficient method for detecting crop rows in agricultural fields to support autonomous field patrolling. Their method employed incremental search techniques to approximate the optimal region of complex data points, combined with the DIRECT algorithm for global optimization. The approach was tested on a hybrid dataset derived from the Hough transform and was designed to detect two or three crop rows. The results showed that the method could accurately detect crop rows, with detection times remaining within acceptable limits. Malavazi et al. (2018) developed a navigation approach for autonomous robots operating in agricultural fields using LiDAR data. In this method, the robot does not require prior knowledge of crop row characteristics such as row size or width. Instead, it determines its path using the PEARL algorithm, which extracts lines from a two-dimensional point mass. To improve crop-row detection for the Oz weeding robot, the authors introduced several modifications and filters to the PEARL algorithm, including outlier penalization, a new model-search step, and the addition of a geometric constraint.

The number of patients with mental disorders is increasing worldwide. Animal experiments, particularly those involving rats, play an important role in the development of sedative drugs. In such experiments, animals exhibiting mental disorders are studied, and these disorders are typically induced through genetic manipulation, brain surgery, or the injection of drugs. Another method for inducing mental disorders in animals involves the use of a small mobile robot equipped with an automated control system. Ishii et al. (2012) investigated mental disorders in rats by inducing stress during adolescence. In their study, stress was generated using a chasing robot that approached adult rats and was equipped with an image-processing system for automatic tracking. Robots can also serve as effective tools in animal behavioral research, particularly when they are capable of entering a group of animals and being accepted for interaction. Such systems are valuable for studying social behavior in animals. Gribovskiy et al. (2018) evaluated the use of an autonomous mobile robot to investigate the group behavior of domestic chicken. The objective of their study was to gather the chickens and enable the robot to act as a leader. The robot successfully performed this role. It received real-time information about both its own position and the positions of the chickens through an external vision system and a microphone. The output of the visual system was also displayed directly to the user through monitoring screens. Table 1 presents a timeline of advancements in robotic applications for repelling wild animals.

Safe route planning involves identifying and avoiding obstacles from the start point to the target. It is the central function of navigation methods. Accordingly, selecting an appropriate navigation technique is the most critical step in robotic path planning (Patle et al., 2019). Farm robots, in particular, must be able to operate well in unstructured agricultural environments (Bechar & Vigneault, 2016). Robot navigation across different environments can be grouped into three categories. The first category is planned motion, in which the robot operates in a known environment that has been mapped in advance (Asefpour Vakilian & Massah, 2017). For example, Sudhakara et al. (2018) proposed the enhanced artificial potential field (E-APF) method for robotic path planning by integrating a grid-based approach with the artificial potential field technique. This algorithm provided an accurate representation of the mobile robot's workspace and performed well in both simple and complex environments while minimizing navigation time. Adeodu et al. (2019) developed a mobile robot for automated plant irrigation. Their system used XBee wireless communication to connect the robot to a soil-moisture measurement module. The robot navigated between plants using a tracking algorithm on a white surface, supported by two infrared sensor modules. This approach enabled the robot to maintain an appropriate distance from crop rows during irrigation, addressed limitations of fixed irrigation systems, and required less space. The second category is random motion, where the robot has no prior map or predefined plan of the environment and instead searches for the target or a

feasible path in a random manner. Because this approach can require substantial time and energy to locate a target, it is generally better suited to large mobile robots with access to significant energy resources. In this context, Al-Muhammed and Abu Zitar (2018) introduced an algorithm that combines random search techniques with effective mapping and dynamic adjustment of search behavior to discover complex mathematical functions. Their method was reported to be efficient, robust, and time-effective, with the ability to update its parameters and modify its mapping mechanism based on knowledge gained from previous iterations.

The third category of robot navigation is exploration, which occurs in unfamiliar environments and includes heuristic, innovative, and probabilistic methods. In the heuristic method, the robot searches for its target in an unknown environment using various algorithms. As it moves, it creates a roadmap that records previously visited locations. Obstacles and objects detected by the robot's sensors are stored in memory, enabling the robot to gradually understand and navigate its surroundings. In the innovative method, the robot explores the environment in a similar manner but relies on specialized sensing equipment, such as thermal cameras for detecting living targets or proximity sensors for obstacle avoidance. This approach requires less time and energy than heuristic exploration (Vallvé & Cetto, 2015) and is therefore suitable for small rescue robots that must accomplish their tasks within a limited timeframe (Kulich et al., 2017). In the probabilistic method, the robot estimates its current position and the optimal path by calculating the probability associated with each possible route. The robot then selects the path with the highest likelihood of reaching the target. For example, Vroegindeweij et al. (2016) proposed using the intelligent PoultryBot robot for egg collection from laying hens. To operate effectively inside nests, PoultryBot used probabilistic localization via particle filtering to determine its position. They evaluated the estimated paths using Euclidean distance relative to the ground-truth positions obtained from the entire station. The system achieved an accuracy of 0.37 m and an average error of 0.2 m, which was considered acceptable for this application. Kulich et al. (2017) introduced a greedy randomized adaptive search procedure (GRASP) meta-heuristic for addressing the graph search problem (GSP) in unknown navigation environments. This approach computes high-quality solutions rapidly and integrates them within a general navigation framework. Their method demonstrated promising results in simulation, generating near-optimal solutions in approximately 1 second. The framework was evaluated across four maps and 1200 experiments, with findings confirming that the proposed strategy is both effective and practical. Massah et al. (2021) designed a robotic farmer-assistant platform equipped with machine-vision systems to evaluate kiwifruits before harvest without damaging the fruit. The robot traveled along kiwifruit trellises to estimate yield. Several image-based features, including intensity histograms, histograms of oriented gradients, shape context, and local binary patterns, were extracted from captured images, and the number of kiwifruits was predicted using a support vector machine (SVM).

Therefore, the objectives of this study are: (a) to design and develop a tracking system for a farm guard robot, and (b) to develop an image-processing approach for detecting moving objects that represent attacking animals. Common invasive animals in agricultural fields, such as white-tailed deer, birds, kangaroo rats, and wildlife from the Hyrcanian forests of northern Iran, often exhibit unpredictable movement patterns and nocturnal activity, which can lead to significant crop damage (Vijayan & Pati, 2002; Craven & Hygnstrom, 1994; Howard, 1994; Meinecke et al., 2018; Nabi et al., 2009). The robot's detection algorithm was designed to identify moving objects representing such animals. However, the system was evaluated using a remotely controlled replica to simulate animal behavior. Specific characteristics such as animal size, speed, and nocturnal activity were not directly incorporated into the testing process, although these factors could be considered in future system improvements.

## MATERIALS AND METHODS

### *Development of the robotic tracked carrier*

The robot measured 850 mm in length, 850 mm in width, and 600 mm in height from the ground surface. These dimensions were selected to enable effective tracking and repelling of wild animals in agricultural fields. In the mechanical design, a safety factor greater than 2.5 was considered to ensure structural reliability. The robotic framework was modeled using SolidWorks 2013 (Dassault Systèmes, France). The robot structure can be divided into two main sections: (a) the carrier and tracked system, and (b) the devices and instruments used to scare off attacking animals. As illustrated in Fig. 1, the overall structure of the carrier and tracked system consists of the following main components:

Chassis (part 1): The robot's main chassis was made of 20 mm × 20 mm St37 steel profile, which could be machined.

Tracked system (part 2): In order to obtain more friction with the ground and to gain more traction than the plastic wheels.

DC electromotors (part 3): The tracked system was driven by two DC motors with a maximum power output of 500 W, whose power was transmitted to the spiral gearboxes.

Spiral gearboxes (part 4): To increase the torque by the gearbox (SSN40-1MDAR, Lenze, Germany) ratio ( $i = 15$ ).

Battery (part 5): The robot's power supply was two 12V, 28 Ah lead-acid batteries (FARA1228, Faratel, Iran).

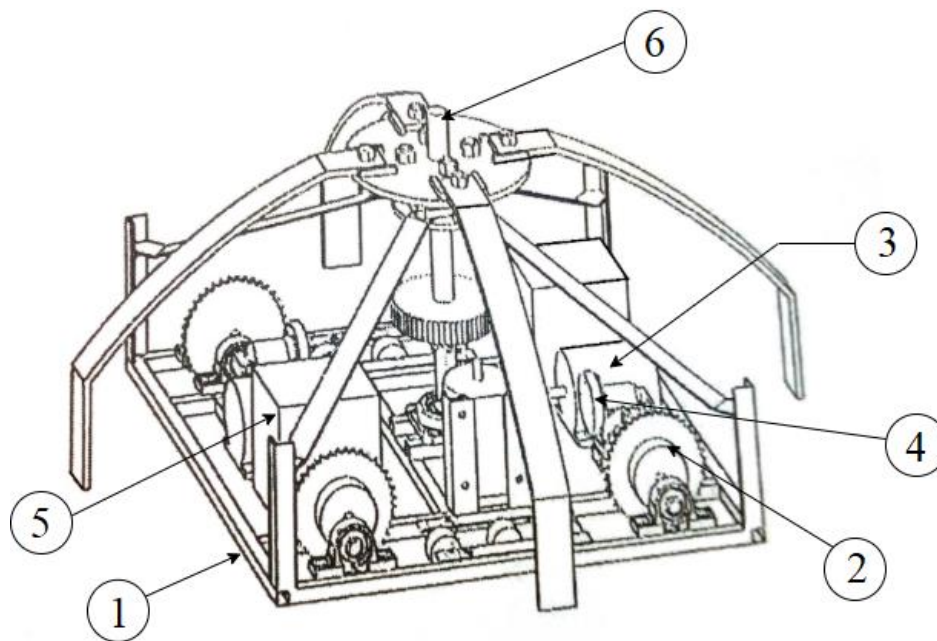
Rotary central shaft (part 6): This shaft rotates the robot's blades, powered by a DC electromotor.

Table 2 shows the mechanical specifications of the robotic tracked system.

Furthermore, devices and instruments to scare the attacking animals are shown in Fig. 2, including (1) flashers, (2) sprinklers to spray odorant fluids to repel sensitive animals, (3) a beeper to produce a loud noise, and (4) rotating blades.

**Table 1.** A timeline of progress in robotic applications in repelling wild animals

Study	Reference
A robot acts as a herd dog to control a bunch towards a specific location	Vaughan et al. (2000)
AgBo robot to guard farmlands through crop rows	Grift (2007)
Prey-bearing microrobots to control the behavior and motility of crickets and to create a controlled dynamic interaction with insects	Guerra et al. (2010)
Fish-shaped robots to study the behavior and reaction of fish in water	Aureli et al. (2012)
Robotic self-propelled fish to achieve a more flexible movement in water	Yu et al. (2014)
A data-driven motion control method for a robotic fish to achieve optimal movement in water	Ren et al. (2015)
Design and modeling of a three-dimensional motion of a robotic dolphin for diving to a depth of 300 m	Yuan et al. (2017)
The Sphero intelligent robot controls the direction and speed of rats' movement in a realistic behavioral environment	Gianelli et al. (2018)
An intelligent robot to protect and prevent pets from being harmed	Chrzanowski et al. (2019)



**Fig. 1.** The robot's main components.

**Table 2.** Specifications of the robotic tracked system

Parameter	Value
Total weight (N)	500
Tracked length (Soil-engaging length) (cm)	70
Tracked width (Soil-engaging width) (cm)	5.5
Travel speed (cm/s)	21
Diameter of chain wheels (cm)	12.8
Pitch of chain wheels (cm)	3.9
Number of chain wheels (both sides)	4
Number of boogie wheels (both sides)	6

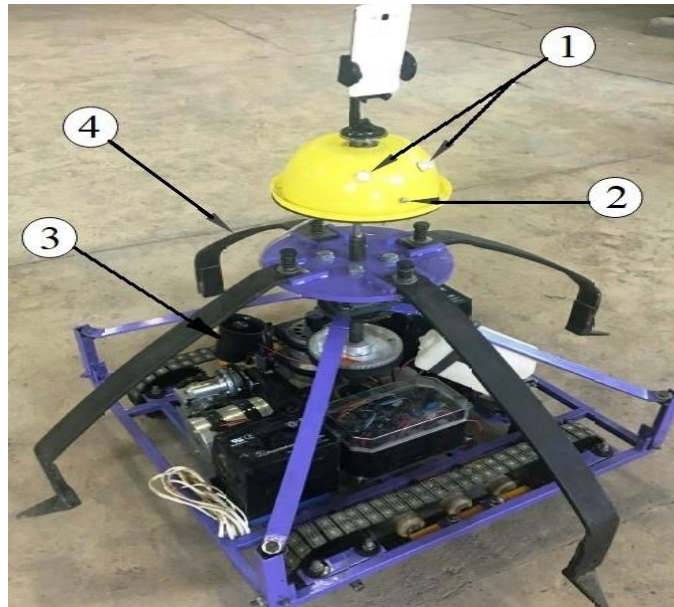


Fig. 2. Devices and instruments to scare the attacking animals.

*Navigation and data processing*

To control the robot’s displacement, a simple closed-loop feedback control system was applied (Fig. 3). The automatic tracking system, integrating GPS (NEO-6M, u-blox, Switzerland) and machine vision, enabled the robot to navigate toward designated targets. An experimental field located at the College of Abouraihan, University of Tehran, was selected for testing. The geographic coordinates (latitude and longitude) of the four field corners, along with predefined in-field control points for path planning, were determined (Fig. 4). Based on these control points, the robot traversed the field using a snake-pattern algorithm (Fig. 5). At specified intervals, it stopped to capture images and perform image processing. For image acquisition, an Android-based mobile phone camera was employed for convenience. The camera was connected wirelessly to a laptop via DroidCamX (Wireless Webcam Pro, Version 6.5). It was mounted vertically on a holder to capture environmental images. To obtain a complete view of the surroundings, the camera rotated 360° at predefined intervals. This rotation was achieved using a stepper motor (EM-242/STH-39H112, Shinao, China), onto which the camera holder was mounted (Fig. 6). All captured images were stored in the laptop’s memory

for subsequent processing. A flowchart illustrating the integration of these components with the robot is presented in Fig. 7. When consecutive image processing detected a moving object within the field, the robot altered its direction and pursued the object while avoiding contact with crop rows. The coordinates of the crop rows had been predefined in the GPS system, enabling safe navigation. Considering typical GPS positional errors (approximately 3–15 m), predefined safety margins were incorporated to maintain a minimum distance from crops, thereby preventing plant damage during maneuvering (Fig. 4). The snake-pattern algorithm ensured comprehensive field coverage during routine patrol. However, upon object detection, the navigation system dynamically adjusted the robot’s trajectory to pursue the target, thereby simulating adaptive responses to erratic animal movements reported in wildlife behavior studies (Ishii et al., 2012). Although the robot’s movement does not explicitly replicate species-specific trajectories (e.g., random foraging patterns of deer or birds), the GPS-based redirection mechanism provides real-time adaptability and avoids rigid, predefined motion paths. The robot operating in an agricultural field is shown in Fig. 8.

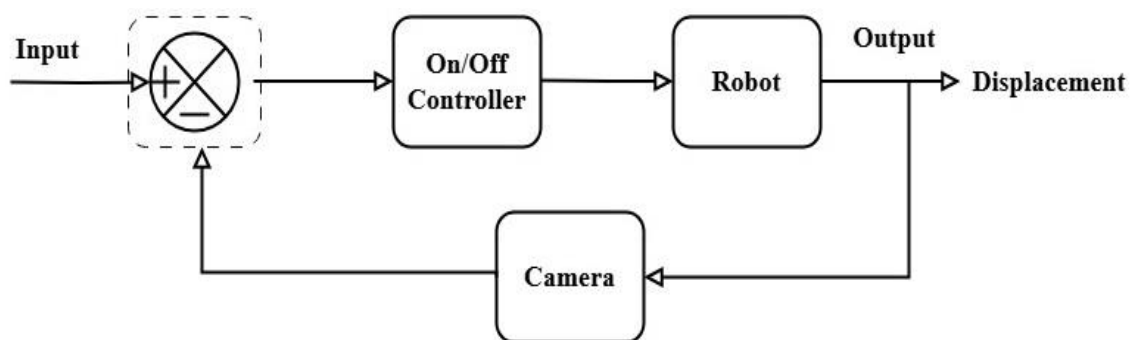


Fig. 3. The block diagram of the closed-loop control system of the robot.

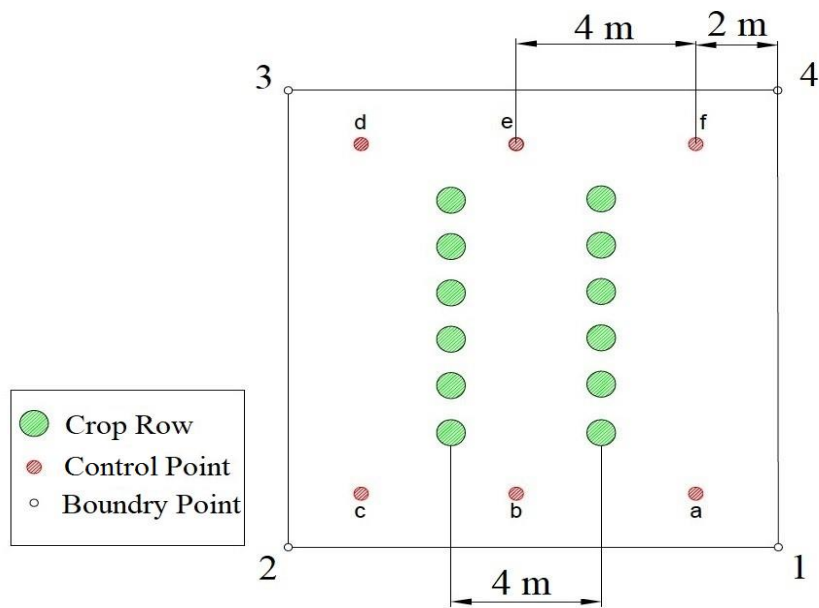


Fig. 4. Schematics of the experimental field and its control points for tracking the robot.

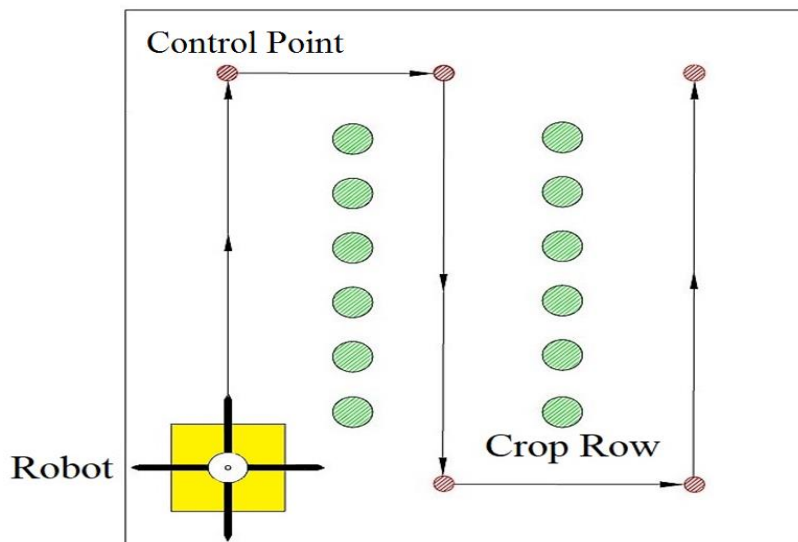


Fig. 5. Robot using snake algorithm in field.

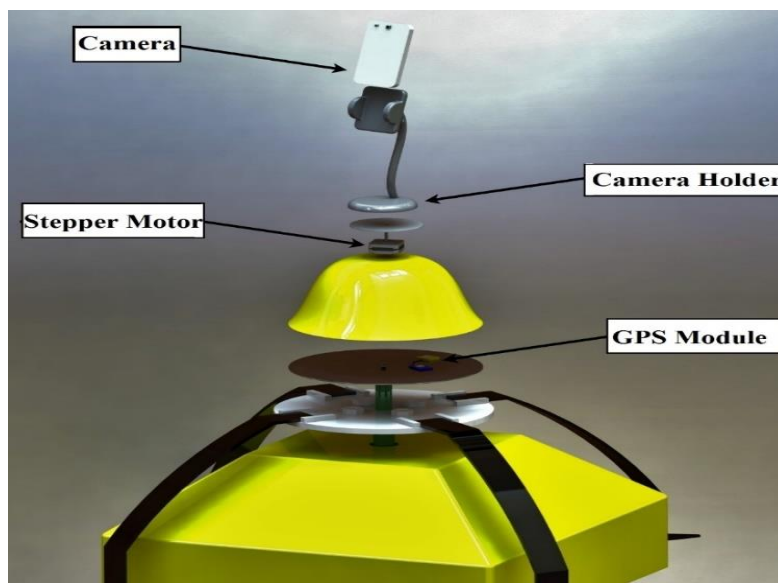


Fig. 6. Components of the image acquisition unit of the robot.

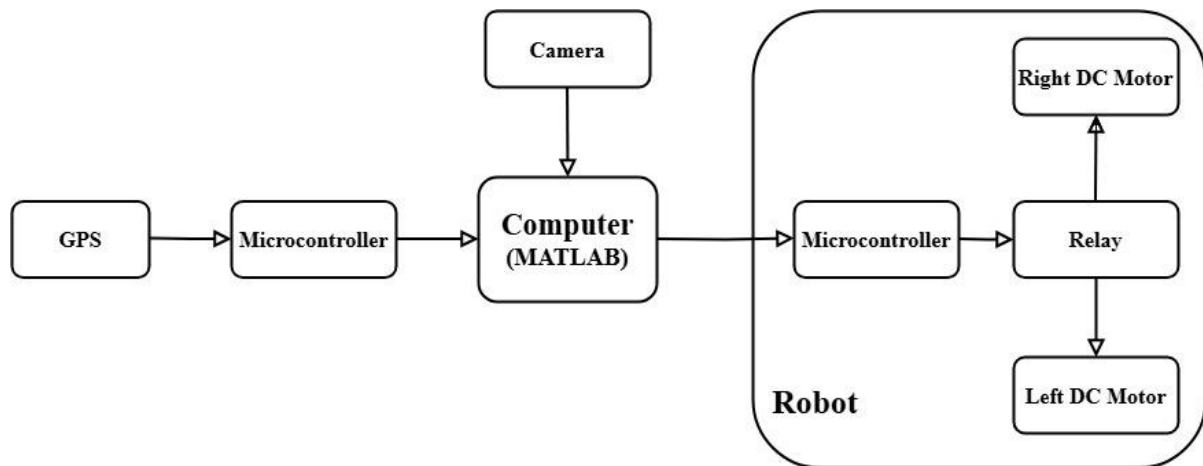


Fig. 7. Flowchart showing how to connect tracking equipment to the robot.



Fig 8. The robot in an agricultural farm.

During the robot's movement toward the target, its current position (latitude and longitude) was continuously compared with the target's coordinates in real time. As long as the robot's coordinates approached those of the target, it continued moving in a straight line to reduce the distance to the object. However, if the GPS coordinates indicated that the robot was moving farther from the target, the control system recognized that the robot was deviating from the desired path and redirected it toward the target. Fig. 9 illustrates the general algorithm governing the robot's movement within the field for detecting and repelling attacking animals.

#### Image processing algorithm

The object-detection algorithm used images captured by the robot's camera from eight directions around the robot, each separated by a 45° angle. In each direction, two images were captured with a 2-second interval between them. Each captured image was then divided into six equal sections for analysis. Fig. 10 presents the algorithm used in the robot's image-processing system to detect animals. First, the red, green, and blue (RGB) bands of the captured images were extracted. The

gray-level differences between the corresponding sections of the two consecutive images were then calculated. In the next step, the normalized standard Deviation of the resulting difference images was computed for each color band, referred to as Standard Deviation of the Red band (SDR), Standard Deviation of the Green band (SDG), and Standard Deviation of the Blue band (SDB). If at least one of these parameters exceeded a predefined threshold value ( $a\%$ ) (e.g., 15%), the system interpreted this change as the presence of an animal in that section of the image.

To determine the most effective detection approach, two additional color models, Hue, Saturation, Value (HSV) and *Lightness, a, b* (Lab) were also evaluated alongside the RGB Red, Green, Blue (RGB) model, and their performance results were compared.

All image-processing operations were performed using MATLAB 2010b running on a laptop computer equipped with a 3.4 GHz processor, 12 GB RAM, and a 64-bit Windows 10 operating system.

#### Performance evaluation of the robot

Since the robot relied on a GPS receiver for accurate navigation and path tracking within the field, the first

stage of the study focused on evaluating GPS performance under various climatic conditions. The objective was to determine how different weather conditions affected the robot's operational accuracy.

First, the GPS was assessed for its ability to determine the robot's current position (latitude and longitude) under different climatic conditions. Next, its performance in identifying predefined control points was evaluated. For this purpose, three in-field control points (A, B, and C) were arbitrarily selected, and their geographic coordinates were recorded. Each control point was tested with five replications, and the recorded coordinates were averaged across the five trials. The mean deviations were then calculated, and the differences between the averaged measured latitude and longitude values and the reference coordinates were determined, for example at point A.

Finally, the robot's navigation performance was evaluated by commanding it to move from control point A to control point B under different times of day and

weather conditions. To conduct this assessment, the control points and crop rows in the experimental field were marked according to the pattern shown in Fig. 4, and their latitude and longitude were provided to the robot via its onboard GPS receiver. Experiments were carried out under nine different conditions, comprising three weather types (sunny, partly cloudy, and cloudy) and three time periods (morning, noon, and afternoon).

To evaluate the performance of the robot's image-processing algorithm, the normalized standard deviation threshold for each of the red, green, and blue bands in the detection algorithm shown in Fig. 10 (parameter  $a$ ) was varied from 5% to 30%, with 20 replications conducted for each value. The images saved and processed in MATLAB were analyzed in three color spaces (RGB, HSV, and Lab), and the results obtained at different threshold values were compared to determine the most accurate color space for detecting the unwanted animals.

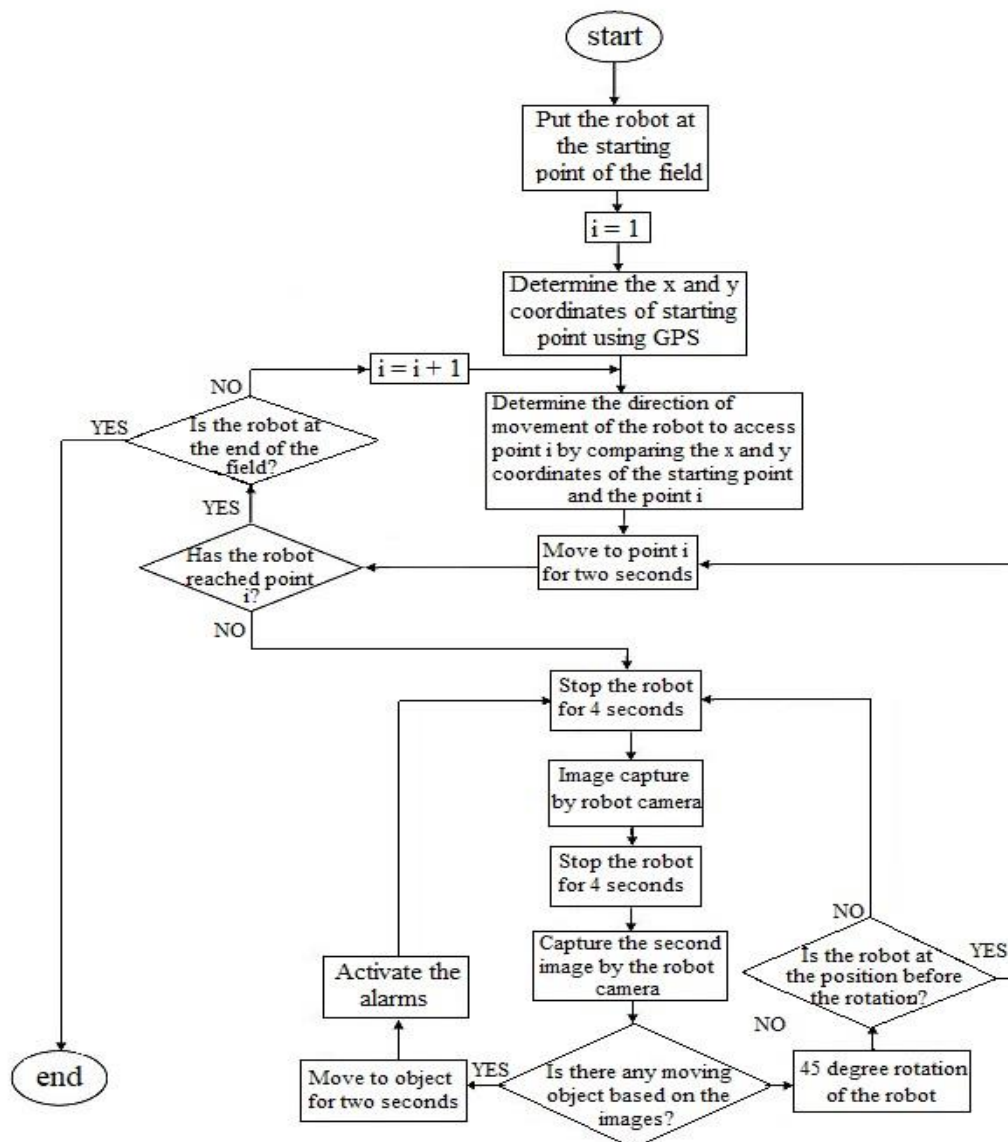


Fig. 9. The proposed algorithm to move robots towards the attacking animals.

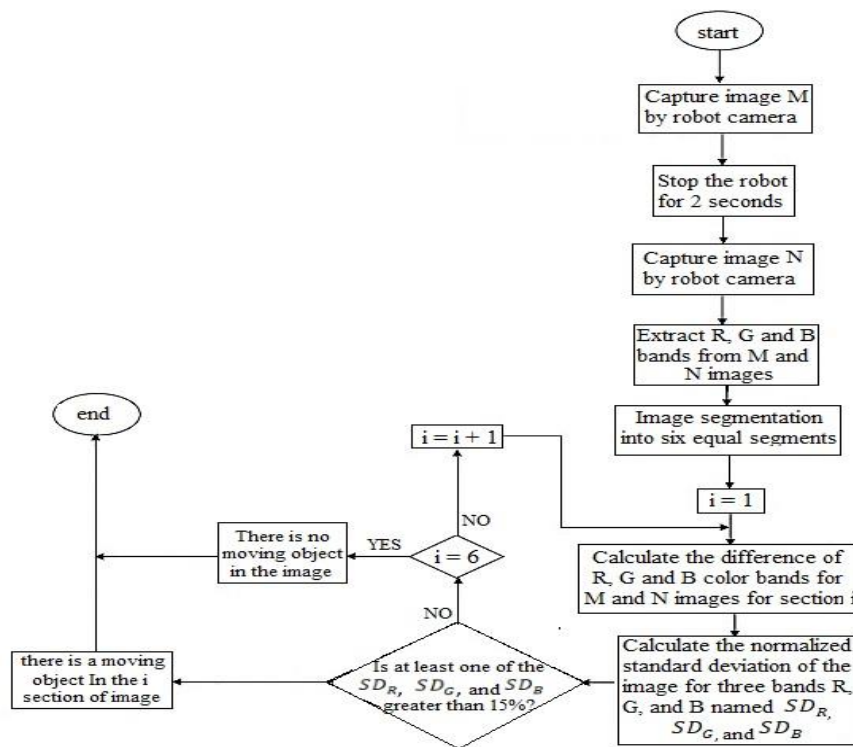


Fig. 10. An algorithm for an image processing system for detecting animals by a robot.

To minimize potential crop damage caused by intruding animals, the robot needed to detect the attacker with its camera as quickly as possible. Therefore, the first step in evaluating the robot’s animal-repelling performance was to measure the image-processing time required for detection in each of the RGB, HSV, and Lab color spaces. Next, the influence of weather and time conditions on the robot’s ability to detect and repel an attacking animal was assessed. Evaluations were conducted under three weather conditions, i.e., sunny, partly cloudy, and cloudy, and two different time periods. For each climatic condition, experiments were performed with five replications. To simulate real attack scenarios, the robot’s performance in detecting and tracking a remotely controlled replica animal was examined. All experiments, including detection and tracking trials, were conducted with five replications to ensure repeatability and reliability of the results.

**RESULTS AND DISCUSSION**

*Performance of the robotic navigation system*

To evaluate GPS accuracy, the time required for the system to detect the robot’s current position was recorded under

each weather and time condition (Table 3). Testing across three different time periods allowed assessment of how varying daylight levels influenced GPS performance. According to Table 3, the average times required for detecting the robot’s current position were approximately 27, 32, and 40 s in sunny, partly cloudy, and cloudy weather, respectively. These results show that GPS performance was highest in clear, sunny conditions. It should also be noted that the time needed for GPS position detection during daylight hours did not follow a strict pattern, as it depended on satellite availability and orbital positioning at the moment of measurement. Table 4 presents the differences between the robot’s measured GPS coordinates and the known coordinates of control point A to assess GPS accuracy in detecting field benchmarks. As shown in the Table 3, weather conditions influenced the GPS’s ability to identify in-field control points, with the system performing better in clear, cloudless weather. Nevertheless, these variations are considered minor given the intrinsic characteristics of GPS technology, which typically exhibits positional errors ranging from 3 to 15 m.

**Table 3.** Evaluation of GPS in different times and weather conditions for the duration of the robot’s current position detection

Weather conditions	Time condition	Required time to detect the robot’s current position (s)
Sunny	Morning	29
	Noon	21
	Afternoon	30
Partly-cloudy	Morning	30
	Noon	32
	Afternoon	34
Cloudy	Morning	40
	Noon	50
	Afternoon	31

**Table 4.** Evaluation of GPS performance in detecting in-field control points at different time conditions and weather conditions for point A

Weather condition	Time condition	Latitude mean difference (min)	Longitude mean difference (min)
Sunny	Morning	0	$1 \times 10^{-5}$
	Noon	$2 \times 10^{-5}$	0
	Afternoon	0	$1 \times 10^{-5}$
Partly-cloudy	Morning	$1 \times 10^{-5}$	$-1 \times 10^{-5}$
	Noon	0	$2 \times 10^{-5}$
	Afternoon	$1 \times 10^{-5}$	0
Cloudy	Morning	$2 \times 10^{-5}$	$-1 \times 10^{-5}$
	Noon	$-1 \times 10^{-5}$	$2 \times 10^{-5}$
	Afternoon	0	$1 \times 10^{-5}$

Evaluating the robot’s performance in moving from in-field control point A to control point B was the most critical component of assessing the tracking system. This evaluation demonstrated the robot’s accuracy in traveling from one predefined location to another and can be considered as a direct measure of navigation precision within the field. Table 5 presents the robot’s performance in moving between control points A and B. As shown in Table 5, when weather conditions change from sunny to cloudy, both the number of GPS errors in detecting in-field control points and the time required to travel between points increase. These results highlight the sensitivity of GPS performance to the atmospheric conditions. Using standalone GPS data is insufficient for accurately navigating the device to a desired position. Therefore, GPS information is typically integrated with additional navigation systems such as an internal navigation system (INS), Doppler velocity log (DVL), or inertial measurement unit (IMU) (Wu et al., 2019). Previous studies have also discussed combining GPS data with techniques such as the Kalman filter, particle filter, LiDAR sensors, SLAM, and Pose SLAM algorithms to enhance positioning accuracy. For this reason, directly comparing the raw GPS data obtained from this robot with results reported in other studies is challenging. A theoretical analysis of the robot’s speed and turning capabilities, based on the 500 W DC motors and a gear ratio of  $i = 15$  estimates a maximum linear speed of approximately 1.5 m/s and a turning radius of 0.85 m, derived from the chassis dimensions and tracked system specifications provided in Table 2. The navigation times recorded between control points (Table 5) indicate that the robot’s movement capability is compatible with moderate-speed animals such as deer (Craven & Hygnstrom, 1994). However, average traversal times increased by approximately 20–30% under cloudy conditions, primarily due to the GPS-related delays.

*Performance of the image processing algorithm*

To evaluate the performance of the robot’s image-processing algorithm, the test results obtained for different values of parameter  $a$  were compared in order to determine the most suitable color space. Fig. 11 illustrates the effect of parameter  $a$  (the normalized standard deviation of the subtracted image) on the accuracy of detecting the attacking animal in different color spaces. As shown in the Fig. 11, the highest detection accuracy was achieved using the RGB color model, with a maximum accuracy of 89% when parameter  $a$  ranged between 10% and 15%. The lowest detection accuracy occurred at parameter values of 5% and 30%. These results indicate that when the difference between two successive images recorded from the same position exceeds 10%, the presence of a moving object can be reliably detected. Differences smaller than 10% may result from external factors such as wind or slight movements of objects within the image and therefore should not be interpreted as evidence of an attacking animal in the field. Similar evaluations were conducted for the HSV and Lab color spaces. Table 6 and Table 7 present the effects of different values of parameter  $a$  (defined as the difference in the normalized standard deviation of the image) on the accuracy of detecting attacking animals in the HSV and Lab color spaces, respectively. According to Fig. 11, the detection accuracy in these color spaces also reaches its maximum when parameter  $a$  falls within the range of 10–15%. As in the RGB case, the lowest detection accuracy occurs at parameter values of 5% and 30%, which can be attributed to the side effects in the image, such as minor object movements. Overall, the RGB color space demonstrated better performance than the other color models for detecting the attacking animals. Therefore, the RGB color space was selected for processing the robot’s camera images, and parameter  $a$  (the difference in the normalized standard deviation of the red, green, and blue bands) was set to 10% as the most appropriate threshold value.

**Table 5.** Robot performance in moving from control point A to control point B

Weather condition	Time condition	Incorrect moves from point A to point B (h)	Required time for moving from point A to point B (h)
Sunny	Morning	2	17
	Noon	3	20
	Afternoon	2	18
Partly-cloudy	Morning	3	18
	Noon	3	19
	Afternoon	4	21
Cloudy	Morning	3	18
	Noon	5	20
	Afternoon	3	21

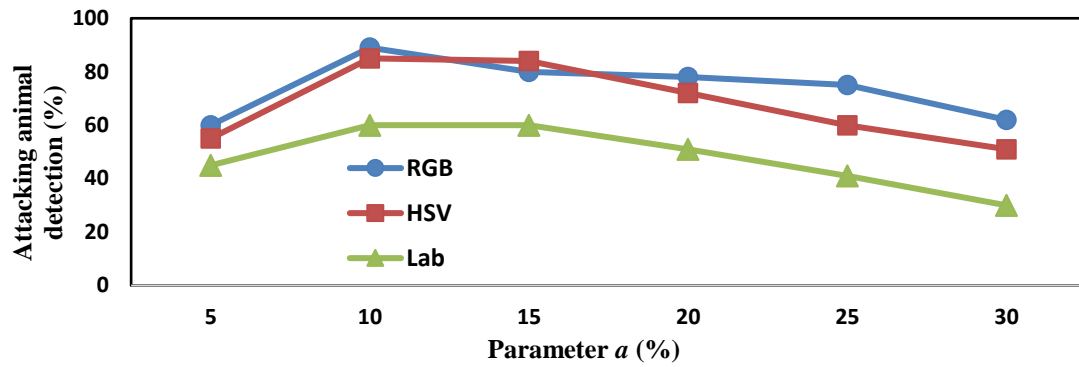


Fig. 11. The effects of parameter *a* on the accuracy of detecting the attacking animal in different color spaces.

Table 6. The effect of parameter *a* on the detection accuracy for the H, S, and V bands

Parameter <i>a</i> (percentage)	Detection accuracy of attacking animals (percentage)
5	55
10	85
15	84
20	72
25	60
30	51

Table 7. The effect of parameter *a* on the detection accuracy for the L, a, and b bands

Parameter <i>a</i> (percentage)	Detection accuracy of attacking animals (percentage)
5	45
10	60
15	60
20	51
25	41
30	30

*Performance of the robot in the detection of attacking animals*

In animal detection, the amount of time spent on detection is one of the most important parameters. Table 8 presents the image-processing time for the robot’s recorded images in three different color models. As shown in Table 8, the RGB color space had the shortest processing time among the evaluated color models, requiring 1.1 s to analyze the images captured by the robot’s camera and transmitted to the computer. Table 9 presents the results for correctly detecting a moving animal replica as an attacking animal under different climatic and lighting conditions. According to Table 9, the robot performed best in detecting and moving toward the object under sunny and partly cloudy conditions with adequate lighting. Under these conditions, the robot successfully detected 4 out of 5 simulated animal attacks. These results indicate that weather conditions and reduced environmental light can have a direct negative effect on the robot’s performance.

*Limitations and future works*

The system’s dependence on visible light captured by the mobile phone camera limits its effectiveness in low-light or nocturnal conditions, when many invasive animals, such as deer and rodents, are most active (Craven and Hynstrom, 1994; Howard, 1994). As shown in Table 9, evaluations conducted under cloudy weather demonstrated reduced detection accuracy, with average detection times increasing

by approximately 48% compared to sunny conditions. These findings highlight the need for integrating infrared or night-vision cameras in future iterations of the system, potentially in combination with Light Detection and Ranging (LiDAR) to enable light-independent navigation (Malavazi et al., 2018). Furthermore, future developments could incorporate animal-specific behavioral models powered by advanced Artificial Intelligence (AI) techniques to improve pursuit efficiency and overall responsiveness to different species.

*Comparative analysis with recent systems*

To contextualize the performance of the intelligent field-guard robot, its capabilities were compared with three recent and relevant studies on automated wildlife intrusion detection and crop protection. Reddy et al. (2023) developed a stationary camera-based system using a 2D-CNN pipeline implemented within a low-cost Internet of Things (IoT) prototype, with cloud-based alerting via Amazon Web Services Simple Email Service (AWS SES). Their system achieved a detection accuracy of 96.78% with an average processing cycle of approximately 3.24 min. However, the system operates as a fixed monitoring node and lacks both mobility and active animal-repulsion mechanisms. Thenmozhi et al. (2025) proposed an Arduino-based solution integrating Passive Infrared (PIR) and ultrasonic sensors with Global System for Mobile Communications (GSM) notifications and basic sound and light deterrents. While this approach emphasizes affordability and practicality for small-scale farms, the

study does not report detailed quantitative metrics for detection accuracy or repulsion effectiveness. Deepika et al. (2024) demonstrated the deployment of a YOLOv8 model on edge hardware (ESP32-CAM using Edge Impulse), achieving a detection accuracy of 96.3% with an inference latency of approximately 20 ms. This work highlights the feasibility of running optimized deep-learning models on resource-constrained devices, although the system remains stationary in its primary mode of detection.

In contrast, the distinguishing features of the present system include integrated mobility via GPS-guided snake-pattern patrolling and autonomous pursuit upon detection, a lightweight image-processing pipeline based on RGB frame differencing with a 10% normalized standard deviation threshold, and multi-modal physical

deterrence (flashers, sprinklers, beeper, and rotating blades) validated in field trials. Under sunny and partly cloudy conditions, the system achieved approximately 89% detection accuracy, an average response latency of 1.1 s, and an empirical repulsion success rate of 80% (4 out of 5 trials). Given the substantial differences in hardware platforms, deployment modes (mobile vs. stationary), and evaluation protocols, direct numerical comparison with previous works is limited. Therefore, the comparative analysis emphasizes practical trade-offs: (1) active mobility and physical repulsion versus passive alerting, and (2) hardware efficiency and robustness in unstructured field environments versus the higher detection accuracy achievable with more complex edge-AI pipelines that require model compression and specialized tooling (Table 10).

**Table 8.** Computer-assisted image processing time in different color models

Color model	Processing time (s)
RGB	1.1
HSV	1.5
Lab	1.6

RGB: Red, Green, Blue; HSV: Hue, Saturation, Value; Lab: Lightness, a, b

**Table 9.** Robot performance for moving toward the animal in different weather and light conditions

Weather condition	Lighting condition	Number of successful detections of animals
Sunny	Intense light	4
Partly-cloudy	Proper light	4
Cloudy	Slight light	3

**Table 10.** Comparative performance of recent animal intrusion detection and crop protection systems

Study	Detection method	Typical hardware	Mobility	Reported accuracy (as published)	Reported latency/processing	Repulsion/deterrent method	Field-trial status/notes
<b>Current study (this work)</b>	RGB frame differencing (10% normalized SD)	Lightweight camera + microcontroller, GPS, tracked chassis, actuator suite	<b>Mobile</b> (GPS-guided snake path, autonomous pursuit)	~89% (field tests)	~1.1 s (avg response)	Flashers, sprinklers, beeper, rotating blades, multi-modal physical repulsion.	Field-tested (small trials). Designed for robustness & low hardware cost. <b>80% success (4/5)</b> in trials
Reddy et al. (2023).	2D-CNN image pipeline	Camera + server/cloud processing; AWS pipeline for alerts.	<b>Static</b> (fixed camera node)	<b>96.78%</b> (reported). ( <a href="https://www.ijdsr.org">ijdsr.org</a> )	~3.24 min processing/pipeline period (reported). ( <a href="https://www.ijdsr.org">ijdsr.org</a> )	Email alerts (AWS SES). No active mobile repulsion reported.	Reported high detection accuracy; implemented as a stationary alert node. ( <a href="https://www.ijdsr.org">ijdsr.org</a> )
Thenmozhi et al. (2025).	Sensor fusion (PIR + ultrasonic) ± simple image processing	Arduino / low-cost IoT nodes, GSM module	<b>Static</b> (distributed low-cost nodes)	<b>Not reported / not extensive</b> quantitative detection/repulsion metrics in the paper. ( <a href="https://www.grmjournals.us">grmjournals.us</a> )	Near-real-time local triggers (sensor latency), no heavy image processing reported. ( <a href="https://www.grmjournals.us">grmjournals.us</a> )	Sound/light deterrents, GSM notifications.	Emphasizes low cost and practicability for small farms; limited published numerical evaluation. ( <a href="https://www.grmjournals.us">grmjournals.us</a> )
Deepika et al. (2024).	YOLOv8 (edge-optimized)	ESP32-CAM + Edge Impulse (on-device)	<b>Fixed / camera-based</b> (edge node)	~96.3% (reported in their dataset & experiments). ( <a href="https://www.irojournals.com">irojournals.com</a> )	~20 ms per inference reported for their optimized edge setup (reported). ( <a href="https://www.irojournals.com">irojournals.com</a> )	Laser- and laser-based deterrence, and LDR triggers, are described.	Demonstrates that heavy detectors can be compressed/optimized to run on constrained hardware (Edge-Impulse pipeline). ( <a href="https://www.irojournals.com">irojournals.com</a> )

## CONCLUSION

Wild animal intrusion into agricultural fields is a major contributor to the decline in both the quantity and quality of agricultural products, and mitigating the risks associated with animal attacks remains a significant challenge. Alongside traditional deterrent measures such as fencing, a robotic machine-vision system combined with GPS-based tracking can provide an effective and adaptive protection strategy. In this study, an intelligent field-guard robot was designed, made, and evaluated. Results showed that the RGB color model was the most suitable for animal detection due to its faster processing time and its ability to achieve 89% accuracy in identifying moving animals. A normalized standard deviation threshold of 10% in the image-processing algorithm was identified as the optimal value for reliably detecting approaching animals. In performance evaluations of the robot's repulsion capability, the best outcomes were observed under sunny and partly cloudy conditions, with successful detection in 4 out of 5 attack trials. Beyond agricultural fields, the developed robot has potential application in protecting poultry farms, livestock facilities, silos, grain warehouses, and other environments vulnerable to wildlife intrusion.

## FUNDING

The authors declare that no funds were received during the preparation of this manuscript.

## CRedit AUTHORSHIP CONTRIBUTION STATEMENT

Conceptualization: Jafar Massah; Methodology: Jafar Massah and Keyvan Asefpour Vakilian; Software: Soha Sami; Validation: Jafar Massah, Keyvan Asefpour Vakilian, and Soha Sami; Formal analysis: Keyvan Asefpour Vakilian and Soha Sami; Investigation: Jafar Massah and Keyvan Asefpour Vakilian; Resources: Jafar Massah and Iman Jazayeri; Data curation: Jafar Massah and Keyvan Asefpour Vakilian; Writing—original draft preparation: Jafar Massah, Keyvan Asefpour Vakilian, and Iman Jazayeri; Writing—review and editing: Jafar Massah and Soha Sami; Visualization: Jafar Massah; Supervision: Jafar Massah; Project administration: Jafar Massah.

## DECLARATION OF COMPETING INTEREST

The authors have no relevant financial or non-financial interests to disclose.

## ETHICAL STATEMENT

Not applicable.

## DATA AVAILABILITY

All data analyzed and generated during this study are included in this published article.

## REFERENCES

- Adeodu, A. O., Bodunde, O. P., Daniyan, I. A., Omitola, O. O., Akinyoola, J. O., & Adie, U. C. (2019). Development of an autonomous mobile plant irrigation robot for a semi-structured environment. *Procedia Manufacturing*, 35, 9-15. <https://doi.org/10.1016/j.promfg.2019.05.004>
- Asefpour Vakilian, K., & Massah, J. (2017). A farmer-assistant robot for nitrogen fertilizing management of greenhouse crops. *Computers and Electronics in Agriculture*, 139, 153-163. <http://dx.doi.org/10.1016/j.compag.2017.05.012>
- Al-Muhammed, M. J., and Abu Zitar, R. (2018). Probability-directed random search algorithm for an unconstrained optimization problem. *Applied Soft Computing*, 71, 165-182. <https://doi.org/10.1016/j.asoc.2018.06.043>
- Aureli, M., Fiorilli, F., & Porfiri, M. (2012). Portraits of self-organization in fish schools interacting with robots. *Physica D: Nonlinear Phenomena*, 241, 908-920.
- Bapat, V., Kale, P., Shinde, V., Deshpande, N., & Shaligram, A. (2017). WSN application for crop protection to divert animal intrusions in the agricultural land. *Computers and Electronics in Agriculture*, 133, 88-96. <https://doi.org/10.1016/j.compag.2016.12.007>
- Bechar, A., & Vigneault, C. (2016). Agricultural robots for field operations: Concepts and components. *Biosystems Engineering*, 149, 94-111. <https://doi.org/10.1016/j.biosystemseng.2016.06.014>
- Chen, B., Zi, B., Qin, L., & Pan, Q. (2020). State-of-the-art research in robotic hip exoskeletons: A general review. *Journal of Orthopaedic Translation*, 20, 4-13. <https://doi.org/10.1016/j.jot.2019.09.006>
- Chrzanowski, A., Detko, P., & Stefanski, T. P. (2019). Intelligent autonomous robot supporting small pets in domestic environment. *IFAC-PapersOnLine*, 52, 194-199. <https://doi.org/10.1016/j.ifacol.2019.08.070>
- Craven, S. R., and Hygnstrom, S. E. (1994). *Deer. The Handbook: Prevention and Control of Wildlife Damage*, University of Wisconsin: Extension publication G3083.
- Gianelli, S., Harland, B., & Fellous, J. M. (2018). A new rat-compatible robotic framework for spatial navigation behavioral experiments. *Journal of Neuroscience Methods*, 294, 40-50. <https://doi.org/10.1016/j.jneumeth.2017.10.021>
- Grahn, S., Gopinath, V., Wang, X. V., & Johansen, K. (2018). Exploring a model for production system design to utilize large robots in human-robot collaborative assembly cells. *Procedia Manufacturing*, 25, 612-619. <https://doi.org/10.1016/j.promfg.2018.06.094>
- Gribovskiy, A., Halloy, J., Deneubourg, J. L., & Mondada, F. (2018). Designing a socially integrated mobile robot for ethological research. *Robotics and Autonomous Systems*, 103, 42-55. <https://doi.org/10.1016/j.robot.2018.02.003>
- Grift, T. E. (2007). Robotics in crop production. *Encyclopedia of Agricultural, Food, and Biological Engineering*. Retrieved from: researchgate.net
- Guerra, R. D. S., Aonuma, H., Hosoda, K., Asada, M. (2010). Semi-automatic behavior analysis using robot/insect mixed society and video tracking. *Journal of Neuroscience Methods*, 191, 138-144.
- Hashemi, A., Asefpour Vakilian, K., Khazaei, J., & Massah, J. (2014). An artificial neural network modeling for force control system of a robotic pruning machine. *Journal of Information and Organizational Sciences*, 38, 35-41. <https://doi.org/10.31341/jios.2014.38.006>
- Hildreth, A. M., Hygnstrom, S. E., Blankenship, E. E., & Vercauteren, K. C. (2012). Use of partially fenced fields to reduce deer damage to corn. *Wildlife Society Bulletin*, 36, 199-203.
- Howard Jr, V.W. (1994). *Kangaroo Rats. The Handbook: Prevention and control of wildlife damage, cooperative*

- extension division*. Institute of Agriculture and Natural Resources University of Nebraska – Lincoln
- Ishii, H., Shi, Q., Miyaagishima, S., Fumino, S., Konno, S., Okabayashi, S., Iida, N., Kimura, H., Tahara, Y., Shibata, S., & Takanishi, A. (2012). Stress exposure with a small mobile robot, both in the immature and mature periods, induces mental disorder in rats. The Fourth IEEE RAS/EMBS International Conference on Biomedical Robotics and Biomechanics, 24-27 June, Roma, Italy.
- Kouzehgar, M., Tamilselvam, Y. K., Heredia, M. V., & Elara, M. R. (2019). Self-reconfigurable façade-cleaning robot equipped with deep-learning-based crack detection based on convolutional neural networks. *Automation in Construction*, *108*, 102959. <https://doi.org/10.1016/j.autcon.2019.102959>
- Kulich, M., Miranda-Bront, J. J., & Preucil, L. (2017). A meta-heuristic-based goal-selection strategy for mobile robot search in an unknown environment. *Computers and Operations Research*, *84*, 178-187. <https://doi.org/10.1016/j.cor.2016.04.029>
- Malavazi, F. B. P., Guyonneau, R., Fasquel, J. B., Lagrange, S., & Mercier, F. (2018). LiDAR-only based navigation algorithm for an autonomous agricultural robot. *Computers and Electronics in Agriculture* *154*, 71-79. <https://doi.org/10.1016/j.compag.2018.08.034>
- Massah, J., Asefpour Vakilian, K., Shabaniyan, M., & Shariatmadari, S. M. (2021). Design, development, and performance evaluation of a robot for kiwifruit yield estimation. *Computers and Electronics in Agriculture*, 185,1-10. <https://doi.org/10.1016/j.compag.2021.106132>
- Massah, J., & Ghazavi, M. R. (2009). Effect of force control system on power and time consumption of tree pruning machine. *Cercetari Agronomice in Moldova (Romania)*, *42*, 1-7.
- Meinecke, L., Soofi, M., Riechers, M., Khorozyan, I., Hosseini, H., Schwarze, S., & Waltert, M. (2018). Crop variety and prey richness affect spatial patterns of human-wildlife conflicts in Iran's Hyrcanian forests. *Journal for Nature Conservation*, *43*, 165-172.
- Nabi, D. G., Rashid Tak, Sh., Kangoo, K. A., & Halwai, M. A. (2009). Increasing incidence of injuries and fatalities inflicted by wild animals in Kashmir. *Injury*, *40*, 87-89.
- Patle, B. K., Babu L, G., Pandey, A., Parhi, D. R. K., & Jagadeesh, A. (2019). A review: On path planning strategies for navigation of mobile robot. *Defence Technology*, *15*, 582-606. <https://doi.org/10.1016/j.dt.2019.04.011>
- Ren, Q., Xu, J., & Li, X. (2015). A data-driven motion control approach for a robotic fish. *Journal of Bionic Engineering*, *12*, 382-394. [https://doi.org/10.1016/S1672-6529\(14\)60130-X](https://doi.org/10.1016/S1672-6529(14)60130-X)
- Sudhakara, P., Ganapathy, V., Priyadharshini, B., & Sundaran, K. (2018). Obstacle avoidance and navigation planning of a wheeled mobile robot using amended artificial potential field method. *Procedia Computer Science*, *133*, 998-1004. <https://doi.org/10.1016/j.procs.2018.07.076>
- Vallvé, J., & Cetto, J. A. (2015). Potential information fields for mobile robot exploration. *Robotics and Autonomous Systems*, *69*, 68-79. <http://dx.doi.org/10.1016/j.robot.2014.08.009>
- Vaughan, R., Sumpter, N., Henderson, J., Frost, A., & Cameron, S. (2000). Experiments in automatic flock control. *Robotics and Autonomous Systems*, *31*, 109-117.
- Vercauteren, K. C., Lavelle, M. J., & Hygnstrom, S. (2006). Fences and deer-damage management: A review of designs and efficacy. *Wildlife Society Bulletin*, *34*, 191-200.
- Vidović, I., & Scitovski, R. (2014). Center-based clustering for line detection and application to crop rows detection. *Computers and Electronics in Agriculture*, *109*, 212-220. <https://doi.org/10.1016/j.compag.2014.10.014>
- Vijayan, S., & Pati, B. P. (2002). Impact of changing cropping patterns on man-animal conflicts in the gir protected area, with specific reference to the talala sub-district, Gujarat, India. *Population and Environment*, *23*, 541-559.
- Vroegindewij, B. A., IJsselmuiden, J., & Van Henten, E. J. (2016). Probabilistic localisation in repetitive environments: Estimating a robot's position in an aviary poultry house. *Computers and Electronics in Agriculture*, *124*, 303-317. <https://doi.org/10.1016/j.compag.2016.04.019>
- Wu, Y., Ta, X., Xiao, R., Wei, Y., An, D., & Li, D. (2019). Survey of underwater robot positioning navigation. *Applied Ocean Research*, *90*, 101845. <https://doi.org/10.1016/j.apor.2019.06.002>
- Xue, J., Zhang, L., & Grift, T. E. (2012). Variable field-of-view machine vision-based row guidance of an agricultural robot. *Computers and Electronics in Agriculture*, *84*, 85-91.
- Yu, J., Wang, K., Tan, M., & Zhang, J. (2014). Design and Control of an Embedded Vision Guided Robotic Fish with Multiple Control Surfaces, Hindawi Publishing Corporation. *The Scientific World Journal*, 13631296. <https://doi.org/10.1155/2014/631296>
- Yuan, J., Wu, Z., Yu, J., Zhou, C., & Tan, M. (2017). Design and 3D motion modeling of a 300-m gliding robotic dolphin. *IFAC-PapersOnLine*, *50*, 12685-12690. <https://doi.org/10.1016/j.ifacol.2017.08.2251>
- Deepika, R., Shalini, P., Sona Saran, S., Sruthi, S., Suvarnamala, T. & Poongothai, M. (2024). Agro guard edge AI - development of sustainable IoT framework for wildlife intrusion detection. *Journal of Electrical Engineering and Automation*, *6*(4), 325-342. <https://doi.org/10.36548/jeea.2024.4.005>
- Reddy, B. S. V., Deepika, G., Rajendra, M., & Gorijala, L. S. (2023). Animal intrusion detection in fields using convnets-2D with cloud service AWS SES alerts. *International Journal of Scientific Development and Research*, *8*(4), 785-788. <https://ijsdr.org/papers/IJSDR2304137.pdf>
- Thenmozhi, A., Abdullah, A., Saqlain Musthaq, S., Shynu, T., & Mohamed Sameer Ali, M. (2025). IoT-enabled precision animal trespass identification and deterrence system for smart agriculture. *American Journal of Science on Integration and Human Development*, *3*(1), 1-12.